



Simultaneous biosorption of methylene blue and trivalent chromium onto olive stone

M.C. Trujillo^a, M.A. Martín-Lara^{a,*}, A.B. Albadarin^{b,c}, C. Mangwandi^b, M. Calero^a

^aDepartment of Chemical Engineering, University of Granada, 18071 Granada, Spain, Tel. +34 958 243315; Fax: +34 958 248992; email: mariactrujillo@correo.ugr.es (M.C. Trujillo), Tel. +34 958 240445; Fax: +34 958 248992;

email: marianml@ugr.es (M.A. Martín-Lara), Tel. +34 958 243315; Fax: +34 958 248992; email: mcalero@ugr.es (M. Calero)

^bSchool of Chemistry and Chemical Engineering, Queen's University Belfast, Belfast BT9 5AG, Northern Ireland, UK, emails: aalbadarin01@qub.ac.uk (A.B. Albadarin), c.mangwandi@qub.ac.uk (C. Mangwandi)

^cDepartment of Chemical and Environmental Sciences, University of Limerick, Limerick, Ireland, Tel. +44 0 28 9097 4378; Fax: +44 0 28 9097 6524

Received 26 March 2015; Accepted 12 August 2015

ABSTRACT

In this work, olive stone (OS) was utilized to investigate its capacity as biosorbent for methylene blue (MB) and Cr(III), which are usually present in textile industry effluents. Equilibrium and kinetic experiments were performed in batch experiments. The biosorption process followed pseudo-second-order kinetics. The equilibrium data were fitted with several models, but Langmuir and Sips models best reproduced the experimental results. Maximum biosorption capacities were 3.296 mg/g (0.0116 mmol/g) and 4.990 mg/g (0.0960 mmol/g) for MB and Cr(III), respectively. Several operation variables, such as biosorbent mass, flow rate, and initial concentration on the removal of dye and metal, were evaluated in column system. The removal efficiency improved as OS mass increased and decreased when flow rate and initial concentration increased. Also, MB uptake was substantially decreased by increasing the initial concentration of Cr(III), ranging from 6.09 to 2.75 mg/g. These results show that the presence of Cr(III) significantly modifies the biosorption capacity of MB by the OS. These results suggest that OS is a potential low-cost food industry waste for textile industry wastewater treatment.

Keywords: Biosorption; Chromium III; Methylene blue; Olive stone; Wastewater treatment

1. Introduction

Industrial activities produce effluents with a wide range of chemicals. For example, tannery effluents not only contain organic compounds but also inorganic compounds, like dyes and heavy metals [1]. Both pollutants are nonbiodegradable and tend to accumulate in living organisms, provoking several disorders

[2] and high environmental problems. Moreover, these compounds present difficulties to treat them. Dyes have a complex molecular structure which makes them difficult to biodegrade [3], while heavy metals are known to be highly toxic at very low concentrations [4]. Conventional technologies seem to be less effective in the removal of these compounds, especially in the case of dyes, so biosorption emerged as a promising treatment with the advantages of its

*Corresponding author.

operational simplicity, availability of biomass, no nutrients requirements, low cost, and minimization of chemicals and sludges [5,6]. Biosorption has been proved to be a good tool to remove dyes and heavy metals [7,8]. There are numerous studies which use different biosorbent from agricultural wastes, [9] such as orange peel, date pits, or tea waste [10,11], to remove both pollutants. Most of these studies are focused on the treatment of one pollutant or two chemicals in a multicomponent system but of the same type (two heavy metals or two dyes). However, there are few works that deal with the treatment of two different chemicals which has real industrial application, as most of effluents contain dyes and heavy metals [12].

This work evaluates the removal of two typical pollutants of wastewaters from textile industry, such as methylene blue (MB) and trivalent chromium, by olive stone (OS). OS has been demonstrated to be a good biosorbent in the removal of several heavy metals [13–16]. However, its usefulness has not been proved with both pollutants in a binary system. Therefore, the capacity of OS to remove both compounds and the effects of each chemical in the biosorption process are examined in the present study.

2. Materials and methods

2.1. Preparation of biomaterial (OS)

OS was provided by an oil extraction plant “Cooperativa Nuestra Señora del Castillo” located in Vilches, province of Jaen (Spain). The stones were obtained from the separation process of the olive cake with an industrial pitting machine. The solid was milled with an analytical mill (IKA MF-10) and <1.000 mm fraction was chosen for the characterization and biosorption tests without any pretreatment. The particle size for the experiments was 1–0.355 mm. Results of physical–chemical characterization of OS are presented in Table 1.

2.2. Preparation of solutions

Synthetic dye solution was prepared by dissolving weighed amount of MB ($C_{16}H_{18}N_3SCl$) in deionized water and diluted to required concentrations. Cr(III) solutions were prepared by dissolving chromium chloride hexahydrate ($Cl_3Cr \cdot 6H_2O$) in deionized water that was further diluted to obtain desired concentrations of the metal. The main properties of both molecules are presented in Table 2. The pH of the solutions was adjusted with 0.1 N solutions of NaOH and HNO_3 .

Table 1
Physical–chemical characterization of OS [15]

Characteristics of OS	
C %	52.34
H %	7.11
N %	0.03
S %	<0.10
O %	40.47
HW %	12.16
EEB %	0.76
Lignin %	25.68
Holocellulose %	54.70
TC, mgC/L	36.84
TIC, mgC/L	0.02
TOC, mgC/L	36.82
BET surface area, m^2/g	0.163
Internal surface, m^2/g	0.140
External surface, m^2/g	0.022
Total porous volume, cm^3/g	1.84×10^{-3}
Pore diameter, Å	453.02

Notes: HW: hot water extractable compounds; EEB: ethanol–benzene extractable compounds; TC: total carbon; TIC: total inorganic carbon; TOC: total organic carbon.

Cr(III) was analyzed by a flame atomic absorption (AA) spectrophotometer (Perkin Elmer, Model A Analyst 200) and MB was measured by UV spectrophotometry ($\lambda = 664$ nm).

2.3. Batch biosorption studies

2.3.1. pH effect

Before discussing the effect of pH on binary dye–metal solution biosorption onto OS, experiments in absence of biosorbent were performed to test the behavior of the binary solution vs. pH of the medium. A mixture of MB–Cr(III) in the ratio 1:1 (100 mg/L MB + 100 mg/L Cr(III)) was prepared and the pH was varied from 3 to 6 (pH values higher than 6 were not studied to avoid the precipitation of metal). The optimal operational conditions and maximal biosorption capacity for both components separately (Table 3), were obtained from previous studies for MB (data not reported) and for Cr(III) [13]. To determine the effect of pH on the removal of the binary aqueous system, biosorption process was studied varying the pH range of 3.0–6.0. According to the results obtained from the experiments of single component, the following experimental conditions were selected: contact time, 120 min; biosorbent concentration, 10 g/L; and temperature, 25°C.

Table 2
Properties of MB molecule and Cr(III) ion

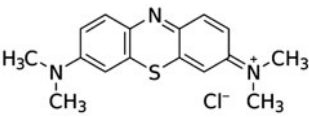
MB		Cr(III)	
Molecular size	13.82 × 5.91 Å	Ionic radius	0.69 Å
Formula	C ₁₆ H ₁₈ N ₃ SCl	Formula	Cl ₃ Cr ₆ H ₂ O
Structure in aqueous solution		Species dissolved in aqueous solution (pH > 4)	Cr ³⁺
Molecular weight in aqueous solution	284.26	Atomic weight in aqueous solution	51.996
Charge	+1	Charge	+3

Table 3
Optimal values of operating parameters and maximum biosorption capacity of MB and Cr(III) onto OS

	MB	Cr(III)
pH	7–8	4
Biosorbent (g/L)	5	10
Particle size (mm)	<1.00	<1.00
Contact time (min)	>60	>50
q_{\max} Langmuir (mg/g)	9.35	5.19

2.3.2. Equilibrium and kinetic biosorption

To study the biosorption of binary dye–metal solution onto OS, the following experimental conditions were taken for equilibrium and kinetic experiments: 1st set of experiments: Cr(III) initial concentration = 100 mg/L and MB initial concentration = 10, 20, 50, and 100 mg/L; 2nd set of experiments: MB initial concentration = 100 mg/L and Cr(III) initial concentration = 10, 20, 50, and 100 mg/L, time = 120 min, and pH 4–5. Samples at fixed time intervals were taken during the kinetic experiment. Although all the experiments have been performed using mass concentration, (as it is worked in industry and expressed in environmental legislation), biosorption capacity results in equilibrium for each pollutants were expressed in molar concentration in order to compare the real uptake.

Cr(III) and MB uptake (q) and percentage of removal (Removal %) were calculated according to Eqs. (1) and (2), respectively:

$$q = \left[\frac{C_i - C_e}{M} \right] \times V \quad (1)$$

$$\text{Removal (\%)} = \left[1 - \frac{C_e}{C_i} \right] \times 100 \quad (2)$$

where C_i and C_e are the initial and equilibrium concentration of Cr(VI) in mg/L, respectively, M is the amount of dry biomass in g, and V is the volume of the Cr(III)/MB solution in L.

2.4. Column biosorption studies

2.4.1. Comparison of single and binary biosorption

Similar to batch experiments, biosorption tests of binary aqueous systems were carried out but in fixed-bed column. The performance of the two components was studied in single and binary solutions. Three experiments were set up with the following conditions: MB initial concentration = 100 mg/L without Cr (III); Cr(III) initial concentration = 100 mg/L without MB; MB and Cr(III) initial concentration = 100 mg/L. The rest of the variables were fixed constant for the three experiments: pH 4, temperature = 25°C, flow rate = 4 mL/min, and mass of biosorbent = 7.5 g. Effluent samples were collected at various time intervals and analyzed.

2.4.2. Effect of different parameters in binary biosorption

Continuous biosorption experiments of binary solutions in fixed-bed column were performed in order to assess the effect of biosorbent mass, initial concentration, and flow rate. The effect of biosorbent mass was investigated with various biosorbent masses of 5.0, 7.5, and 10.0 g. Columns of 22.5 cm of length and an internal diameter of 1.5 cm were used for different bed

depths: 3.7 cm (weight of 5 g), 5.5 cm (weight of 7.5 g), and 8 cm (weight of 10 g). The inlet concentration was 100 mg/L and flow rate was 4 mL/min, in all the cases. The effect of initial concentration was studied using different concentrations of 50, 100, and 150 mg/L. Biosorbent mass and flow rate were held constant at 7.5 g and 4 mL/min, respectively. The influence of flow rate on the removal process was investigated at three different values: 2, 4, and 6 mL/min, at 100 mg/L initial concentration and 7.5 g biosorbent mass. A peristaltic pump was used to pump the solution through the fixed-bed column at room temperature. Samples were collected at regular intervals and the breakthrough curves were obtained at different conditions.

3. Results and discussion

3.1. Batch experiments

3.1.1. Effect of solution pH

Table 3 shows the optimal pH for each single component. For MB dye, the removal was maximum at pH around 7–8. At basic pH, the surface of the biosorbent is negatively charged, thus, strong interactions between cationic dye and the biosorbent take place. According to previous studies, the zero point charge (pH_{zpc}) for OS is around 5 [14]. Thus, the biosorbent carries a negative charge at pH above this value and cationic dyes are best adsorbed beyond this pH_{zpc} [8]. For Cr(III), maximum removal of metal was obtained at pH 4. The retention of trivalent chromium by the OS is mainly due to the ionic attraction between metal ions and the biosorbent carboxylic groups [14,17,18]. For many biosorption systems, it is reasonable to assume that, within a certain pH range, predominantly only one binding site is responsible for sequestering the metal ion. Titrations revealed the predominance of carboxylic groups in the solid samples and they were considered as the only groups responsible for removing lead, as these groups can be negatively charged at pH 4 (pH value of the present study) [14].

The results of the pH effect experiment with the binary solution of dye and metal without any biosorbent are shown in Fig. 1(a). It is observed that from pH value of 4, there are no significant changes in the case of MB. However, with increasing the pH, Cr(III) concentration decreases slightly. This is evident as Cr(III) precipitates at pH values above 6 [19].

Fig. 1(b) shows the results of the biosorption of binary aqueous system onto OS, varying pH. The figure indicates a maximum uptake of the MB at pH 7.0, as it occurs in the single biosorption experiment for component MB (see Table 3). The maximum removal

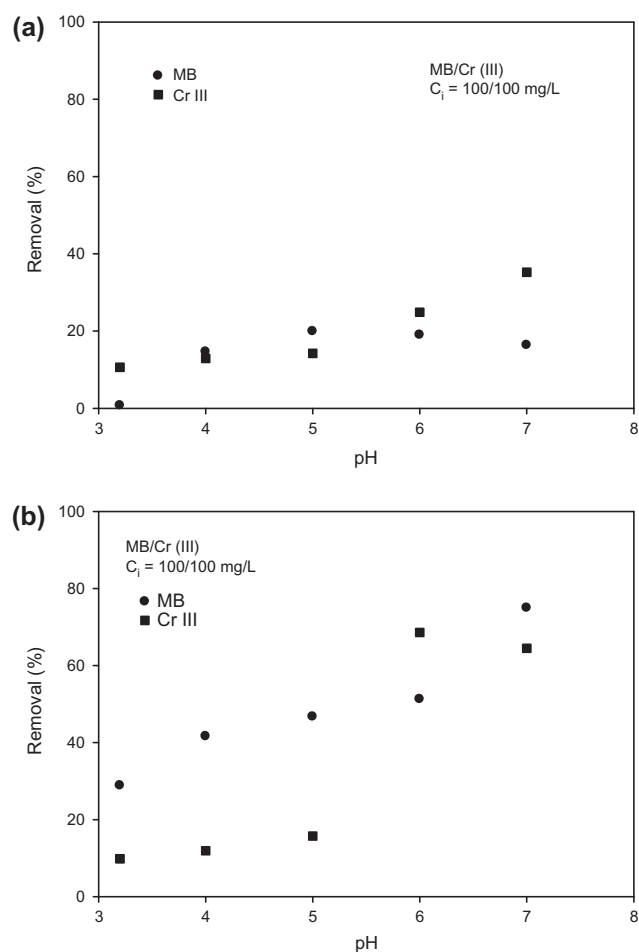


Fig. 1. (a) Effect of pH on MB and Cr(III) without presence of biosorbent and (b) Effect of pH on biosorption of MB and Cr(III) onto OS for binary MB–Cr(III) solutions.

of Cr(III) by OS takes place at pH above 6. As mentioned above, at pH values above 6 Cr(III) precipitates. That explains the high removal levels of Cr(III) in basic medium. Therefore, the optimal pH for the binary biosorption was around 4–5, close to the optimal pH to remove MB, thus preventing the precipitation of Cr(III).

3.1.2. Equilibrium biosorption

Two sets of experiments were performed to assess the influence of the metal on MB biosorption onto OS and vice versa.

Fig. 2 shows that MB uptake increased from 0.638 to 2.75 mg/g, when MB initial concentration varied from 10 to 100 mg/L. However, biosorption capacity of Cr(III) decreased slightly, ranging between 2.78 and 2.24 mg/g.

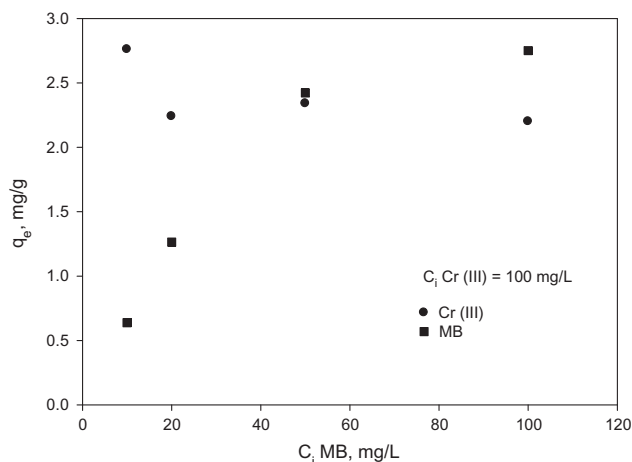


Fig. 2. Biosorption equilibrium capacity of Cr(III) and MB vs. initial concentration of MB.

In the second series of experiments, the biosorption capacity of Cr(III) increased from 0.338 to 2.20 mg/g, when the initial concentration of Cr(III) is raised from 10 to 100 mg/L. However, MB uptake is materially decreased by increasing the initial concentration of Cr(III), ranging from 6.09 to 2.75 mg/g. These results showed that the presence of Cr(III) significantly modifies the biosorption capacity of MB by the OS. Results are shown in Fig. 3.

The equilibrium of the process is represented in Fig. 4 through MB and Cr(III) isotherms for each of the two series of experiments performed. Biosorption capacity in equilibrium (q_e) has been represented versus equilibrium concentration (C_e).

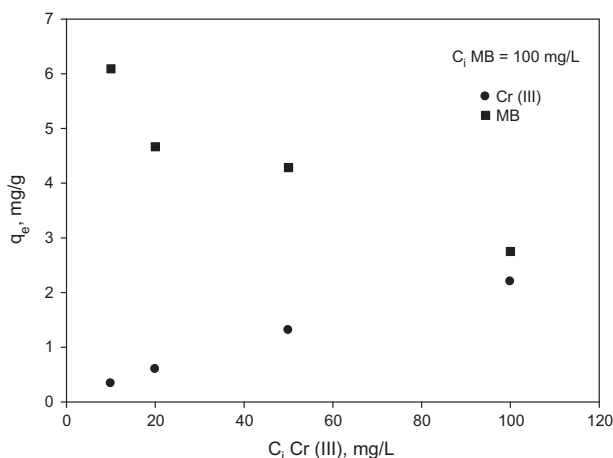


Fig. 3. Biosorption equilibrium capacity of Cr(III) and MB vs. initial concentration of Cr(III).

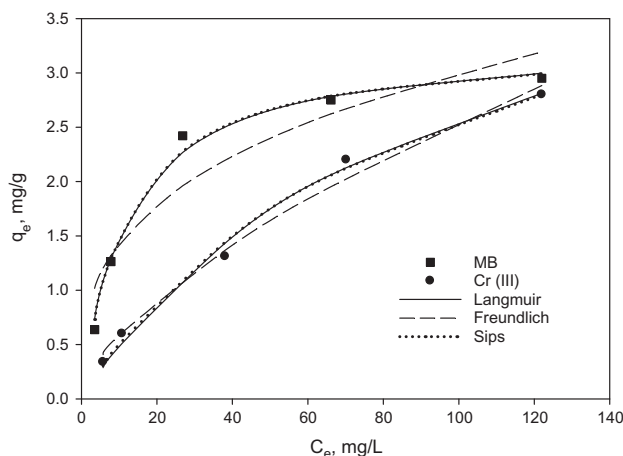


Fig. 4. Isotherms of binary MB–Cr(III) solutions.

In this study, the Sips (Eq. (3)) [20], Langmuir (Eq. (4)) [21], and Freundlich (Eq. (5)) [22] isotherms have been applied in the following nonlinear forms:

$$q_e = q_{\max} \left[\frac{K_s C_e^{n_s}}{1 + K_s C_e^{n_s}} \right] \quad (3)$$

$$q_e = q_{\max} \left[\frac{b C_e}{1 + b C_e} \right] \quad (4)$$

$$q_e = K_F C_e^{1/n} \quad (5)$$

where q_e (mg/g) is the amount of solute adsorbed per unit weight of biosorbent; C_e (mg/L) is the equilibrium concentration of adsorbate in solution; q_{\max} (mg/g) is a constant related to maximum biosorption capacity for a monolayer; b (L/mg) is a constant related to affinity between biosorbent and adsorbate; K_F ((mg/g) (L/mg) $^{1/n}$) and n are the (dimensionless) constants related to the extent of the biosorption, K_s ((L/mg) $^{1/n_s}$) is the equilibrium constant for a heterogeneous solid, and n_s is the Sips isotherm exponent (dimensionless).

The parameter values obtained for the three models used are shown in Table 4.

Langmuir model best reproduces the experimental results in all cases confirmed by Sips model, since in this model the value of n_s is practically 1, and therefore is equivalent to the model of Langmuir.

The maximum biosorption capacity values for MB and Cr(III) are 3.296 and 4.990 mg/g, respectively. This result shows that, in all cases, q_e values for Cr(III) are higher than q_e for MB.

Comparing these results with q_{\max} values obtained for both pollutants in single experiments (Table 3),

Table 4

Langmuir, Freundlich, and Sips models parameters of equilibrium biosorption for binary dye–metal solutions

<i>Langmuir</i>					
	q_{\max} (mg/g)	b (L/mg)	r^2	$\sum (q_{\text{exp}} - q_{\text{cal}})^2$	
MB	3.296	0.0823	1.00	0.0379	
Cr(III)	4.990	0.0106	0.999	0.0312	
<i>Freundlich</i>					
	K_F (mg/g) (L/mg) $^{1/n}$	n	r^2	$\sum (q_{\text{exp}} - q_{\text{cal}})^2$	
MB	0.679	3.10	0.904	0.436	
Cr(III)	0.133	1.56	0.994	0.0465	
<i>Sips</i>					
	q_{\max} (mg/g)	K_S (L/mg)	n_s ((L/mg) $^{1/n_s}$)	r^2	$\sum (q_{\text{exp}} - q_{\text{cal}})^2$
MB	3.271	0.0798	0.98	1.00	0.0335
Cr(III)	5.105	0.0116	1.03	0.999	0.0295

9.35 and 5.19 mg/g for MB and Cr(III), respectively, it is observed that the result for MB in the presence of Cr(III) is significantly lower than q_{\max} for single experiments, while for Cr(III) the difference is not as significant. This suggests that although OS presents a higher biosorption capacity for MB than Cr(III), the influence of Cr(III) over MB is important.

These results indicate that Cr(III) is first bound to OS, avoiding that MB occupies the binding sites. There is a competition between both molecules for the binding sites. On the other hand, MB molecule size is higher than Cr(III), which considerably reduces its possibility of occupying OS pores, favoring the occupation of the pores by Cr(III).

In order to compare these values properly, maximum biosorption capacity of MB and Cr(III) have been expressed in mmol/g, obtaining values for MB and Cr(III) as 0.0116 and 0.0960 mmol/g, respectively. As mentioned previously, for the case of binary solution, biosorption capacity is higher for Cr(III) but when expressing this value in mmol/g, this difference is more marked.

3.1.3. Kinetic biosorption

Figs. 5 and 6 show the biosorption capacity for each period of time (q_t), vs. contact time, for each of the different concentrations of MB and Cr(III) tested.

Comparing the kinetics for both pollutants, it is observed that the biosorption process occurs faster for Cr(III) than MB, since equilibrium is reached prior to chromium. However, increasing the initial concentration, this difference becomes less marked. In fact, at concentration of 100 mg/L no equilibrium is reached (neither for MB neither for Cr(III)) being needed a contact time higher to 120 min.

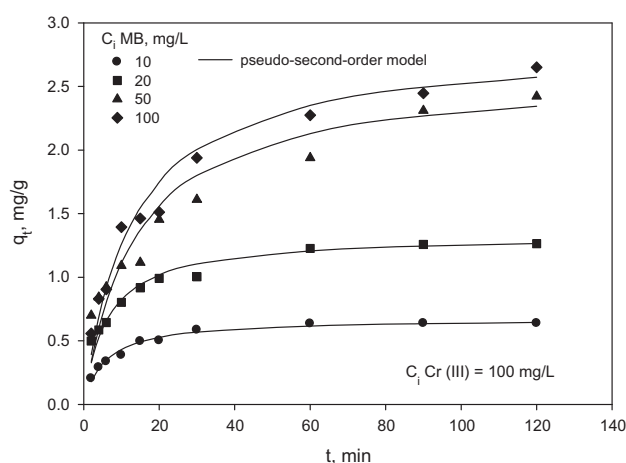


Fig. 5. Biosorption capacity of OS for MB vs. time, in binary solutions.

In order to investigate the mechanism of biosorption, the pseudo-second-order kinetic model was chosen to test dynamic experimental data. This model is used to predict the process behavior in a wide range of operation conditions and it is expressed by the following equation [23]:

$$\frac{dq_t}{dt} = k_{s2} (q_e - q_t)^2 \quad (6)$$

where q_e (mg/g) is the equilibrium biosorption capacity; q_t (mg/g) is the biosorption capacity at time t ; k_{s2} is the pseudo-second-order rate constant of biosorption (g/mg min).

The integral form of above expression is:

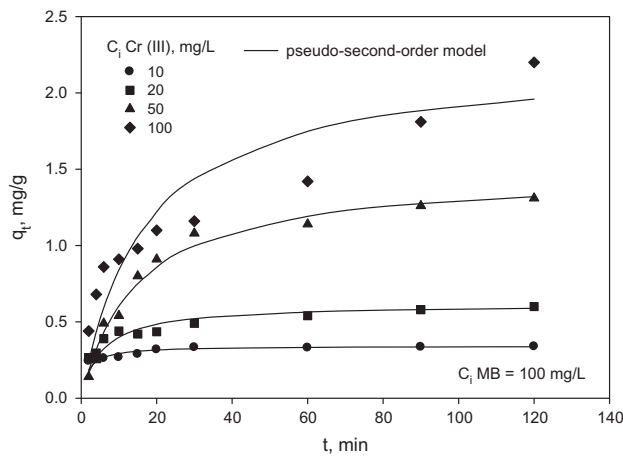


Fig. 6. Biosorption capacity of OS for Cr(III) vs. time, in binary solutions.

$$q_t = \frac{t}{\frac{1}{h} + \frac{t}{q_e}} \quad (7)$$

where $h = k_{s2} q_e^2$ (mg/g min) is the initial sorption rate.

Table 5 shows the values of the pseudo-second-order model parameters for each experiment. According to h , for an initial concentration of 10 mg/L the biosorption process is faster for Cr(III) than MB. However, when increasing the initial concentration of the pollutants the process is reversed, getting an h value of 0.2 and 0.1 mg/g min, for MB and Cr(III), respectively.

However, the pseudo-second-order kinetic constant values indicate that equilibrium is reached faster for Cr(III), for all different concentrations.

As expected, biosorption capacity values increase when increasing initial concentration of the pollutant in both cases, and these values are higher for MB.

3.2. Column experiments

3.2.1. Breakthrough curves

As it can be observed in Fig. 7, breakthrough curves show similar trend when comparing single component solutions with binary solutions. However, breakthrough time was reached sooner in binary aqueous systems. For the case of single-component MB solution, the breakthrough time was attained at 50 min, while for binary solution, it was accomplished around 20 min. Regarding Cr(III), there is no significant difference between single and binary solution as in both cases the breakthrough time was reached in the first ten minutes. However, the exhaustion time was reached faster for the binary system case. As batch experiments indicated, there is a negative influence of the metal on dye biosorption.

Characteristic parameters of the breakthrough curves were obtained according to the following equations proposed in previous works [18,24].

The volume of the effluent at total flow time, can be calculated through the following equation:

$$V_{\text{eff}} = Q t_i \quad (8)$$

where V_{eff} is the volume of effluent (mL), t_i is the total flow time (min), and Q is the volumetric flow rate, (mL/min).

The total mass of solute adsorbed is calculated by Eq. (9):

$$q_{\text{total}} = \frac{Q}{1000} \int_{t=0}^{t=t_i} C_R dt \quad (9)$$

where q_{total} is the total mass of solute adsorbed (mg) and C_R is the concentration of solute removed (mg/L).

The total amount of solute sent to the column until total flow time, can be calculated by Eq. (10),

Table 5
Pseudo-second-order model parameters for binary dye–metal solutions biosorption

	C_i (mg/L)	q_e (mg/g)	h (mg/g min)	k_{s2} (g/mg min)	r^2
MB	10	0.674	0.121	0.267	0.999
	20	1.330	0.217	0.123	0.998
	50	2.607	0.194	0.0285	0.983
	100	2.841	0.227	0.0282	0.994
Cr(III)	10	0.342	0.204	1.742	0.999
	20	0.615	0.114	0.301	0.997
	50	1.480	0.102	0.0466	0.994
	100	2.229	0.135	0.0272	0.945

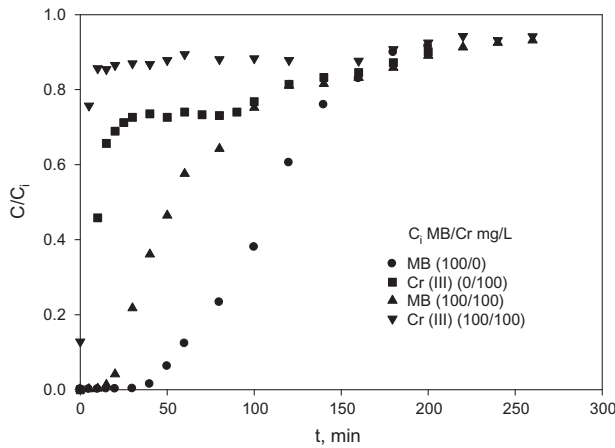


Fig. 7. MB and Cr(III) breakthrough curves in single and binary solutions.

$$m_{total} = \frac{C_i Q t_i}{1000} \tag{10}$$

where m_{total} is the total amount of solute sent to the column (mg) and C_i is the inlet solute concentration (mg/L).

The total solute removal (%R) at total flow time can be calculated from the ratio of total mass of solute adsorbed (q_{total}) to the total amount of solute sent to the column (m_{total}) as follows:

$$\%R = \frac{q_{total}}{m_{total}} \times 100 \tag{11}$$

The adsorption capacity, q_e (mg of solute adsorbed by gram of adsorbent), and the average solute concentration which remains in the effluent solution, C_e (mg/L) can be determined by Eqs. (12) and (13):

$$q_e = \frac{q_{total}}{m} \tag{12}$$

$$C_e = \frac{m_{total} - q_{total}}{V_{eff}} \times 1000 \tag{13}$$

where m represents the mass of the adsorbent (g).

Table 6 shows the results obtained for breakthrough curves of Fig. 7. From a practical point of view, the exhausted time, t_{ex} , is established when the concentration in the effluent is higher than 90–95% of the inlet concentration. The breakthrough time t_b , is established when the metal concentration in the effluent reaches a determined value (related to the permitted disposal limit for each contaminant). Also, the biosorption capacity in mmol/g has been included.

Biosorption capacity (q_e , mmol/g), is very similar when contaminants are single in solution or a mixture of both. However, the removal (%) decreases significantly. Thus, for the MB, the removal percentage is 57.03% when it is the only contaminant present in solution and 31.70% in the MB–Cr(III) mixture. Something similar happens for Cr(III). If the capacity values for the MB biosorption and Cr(III) are compared, it appears that the values are superior for the Cr(III), both when it is alone in solution and when a mixture of both contaminants are present in solution. Nevertheless, the removal percentage is higher for the MB in both cases. This can be explained if the values of breakthrough and exhaustion times are observed. For example, for biosorption test of mixtures of MB/Cr(III), the exhaustion time is 200 min for MB and 60 min for Cr(III).

3.2.2. Effect of initial concentration

The effect of influent concentration of MB and Cr(III) is shown in Fig. 8. It is illustrated that the breakthrough time decreased with the increase in dye concentration. Considering a breakthrough time at $C/C_i = 0.05$, it was reached at 40, 20, and 5 min, at MB concentration 50, 100, and 150 mg/L, respectively. At lower influent dye concentrations, breakthrough curves were dispersed and breakthrough occurred

Table 6
Characteristic parameters of breakthrough curve for MB and Cr(III) biosorption onto OS

C_i MB/Cr(III) (mg/L)	Q (mL/min)	V_{ef} (mL)	q_{total} (mg)	m_{total} (mg)	C_e (mg/L)	q_e (mg/g)	q_e (mmol/g)	R (%)	t_b (min)	t_{ex} (min)
100/0	4	800	45.62	80.0	42.97	6.082	0.0214	57.03	40	180
0/100	4	800	19.58	80.0	75.52	2.611	0.0502	24.48	0–5	180
100/100	4	1,040	32.97	104.0	68.3	4.395	0.0155	31.70	5	200
100/100	4	1,040	18.94	104.0	81.78	2.526	0.0486	18.21	–	60

slower. As initial concentration increased, sharper breakthrough curve was acquired. These results can be due to the fact that more biosorption sites were being covered with the increase in dye concentration. The larger the influent concentration is, the sharper is the slope of the breakthrough curve, and the smaller is the breakthrough time. Higher concentrations produce a higher driving force, which brings on the biosorption process. At lower dye concentrations, flat breakthrough curves were obtained, which means longer mass transfer zone and lower biosorption rates. These results suggest that the fluctuation of concentration gradient affects the saturation rate and breakthrough time [25]. Regarding Cr(III), similar behavior was observed although the breakthrough and saturation time were reached sooner. Steeper breakthrough curves were obtained in the first few minutes, keeping flat until the end of the experiment.

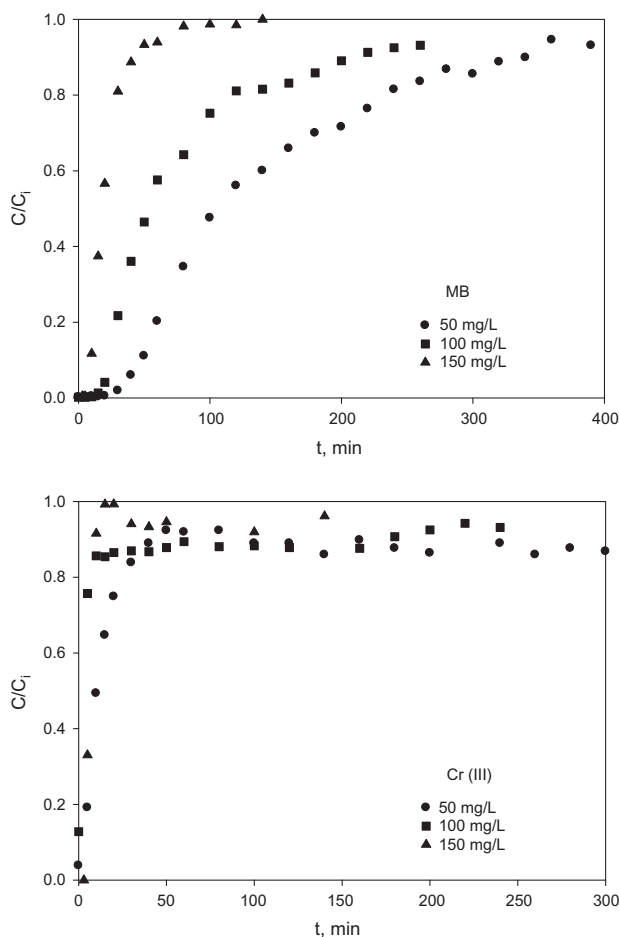


Fig. 8. MB and Cr(III) breakthrough curves at various initial concentrations in binary solutions.

3.2.3. Effect of mass of biosorbent

Experiments were conducted to investigate the effect of biosorbent mass on biosorption capacity. The breakthrough curves, for MB and Cr(III), at different biosorbent mass are shown in Fig. 9. A notable increase in the MB biosorption was observed at higher biosorbent mass (10 g). Considering $C/C_i = 0.05$, the breakthrough times were 10, 20, and 30 min at biosorbent masses of 5, 7.5, and 10 g, respectively. With respect to Cr(III), although the breakthrough time is reached in the first few minutes of operation for all biosorbent masses, the saturation time is attained more slowly as biosorbent mass is increased. As the mass increased, dye and metal molecules have more time to contact with biosorbent, promoting a more efficient removal. The breakthrough curve becomes flatter with increase in biosorbent mass as a result of

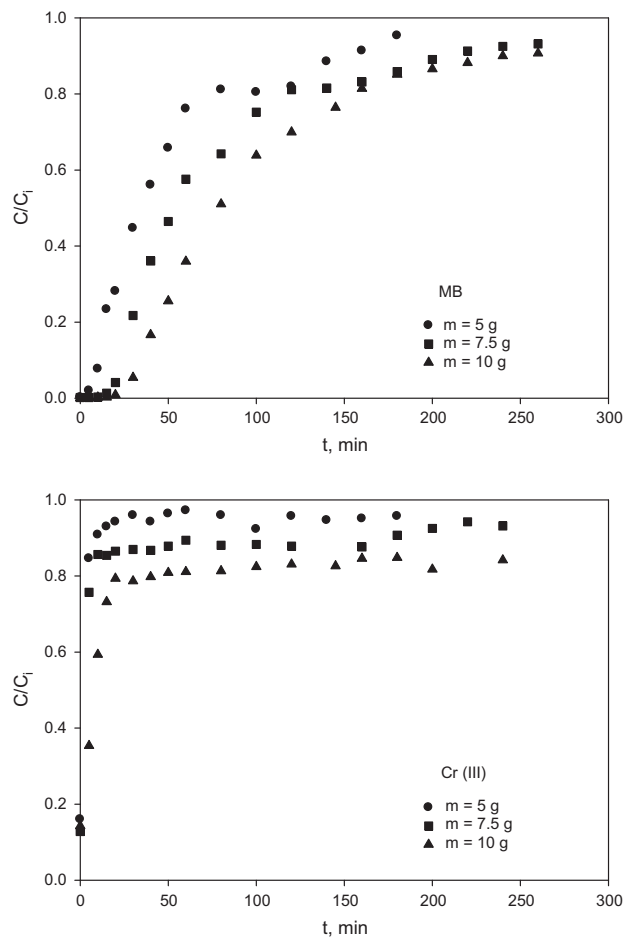


Fig. 9. MB and Cr(III) breakthrough curves at various biosorbent mass in binary solutions.

wider solution movement zone. It was found that higher biosorbent mass results in an increase in the biosorption capacity due to a rise in the surface area of the biosorbent which enhances the availability of biosorption sites [25].

3.2.4. Effect of flow rate

The study of the effect of flow rate suggests that biosorption increases with the decrease in flow rate. Fig. 10 shows the breakthrough curves for MB and Cr(III) at different flow rates. It was observed that, as the flow rate decreased, the breakthrough curve became flatter and the breakthrough time was reached earlier at higher flow rates. Considering $C/C_i = 0.05$, the breakthrough times for MB were 35, 20, and 10 min at flow rates of 2, 4, and 6 mL/min, respectively. In the case of Cr(III), the saturation time is attained in the first ten minutes at flow rates of 4 and 6 mL/min, while it is reached at 70 min at 2 mL/min

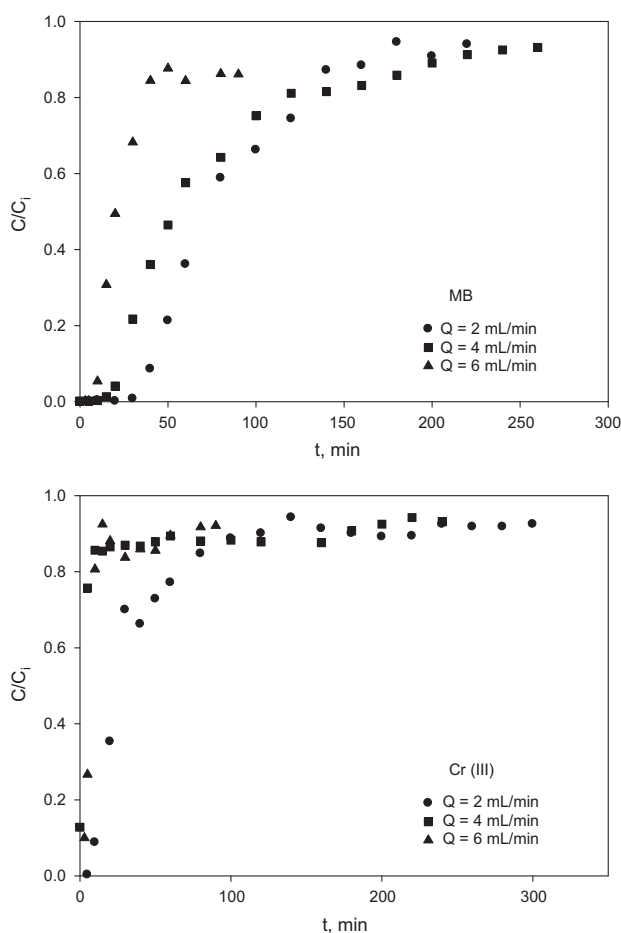


Fig. 10. MB and Cr(III) breakthrough curves at different flow rates in binary solutions.

flow rate. At lower flow rates, diffusion effects are greater as a result of the relative sufficient residence time of the adsorbates in the column which makes them have more time to contact with the biosorbent, favouring the biosorption process. Moreover, the higher turbulence at higher feed flow rate may lead to a weaker interaction and intraparticle mass transfer between the adsorbates and biosorbent [26].

4. Conclusions

The results of this study showed that the optimal pH for biosorption of MB and Cr(III) onto OS, was 8 and 4, respectively. Experimental data were accurately represented by Langmuir, Freundlich, and Sips models, and OS biosorption capacity was found to be higher for the dye than metal. However, Cr(III) interfered in the biosorption of MB, according to batch and column experiments, as a competition for the binding sites occurred between both molecules. Biosorption mechanism was studied by a pseudo-second-order kinetic model, indicating that the process was faster for Cr(III) than for MB. The column experiments showed that the operation variables had an effect in the biosorption and the optimal conditions for the removal of MB and Cr(III) were lower solute initial concentrations, higher bed depth and lower flow rate. The more important variable, in addition to pH, seems to be the initial concentration for MB and flow rate for Cr(III). Therefore, it can be concluded that OS is a potential biosorbent for the treatment of effluents from textile industry.

References

- [1] L. Shakir, S. Ejaz, M. Ashraf, N. Ahmad, A. Javeed, Characterization of tannery effluent wastewater by proton-induced X-ray emission (PIXE) analysis to investigate their role in water pollution, *Environ. Sci. Pollut. Res.* 19 (2012) 492–501.
- [2] M.A. Al-Ghouti, J. Li, Y. Salamh, N. Al-Laqtah, G. Walker, M.N.M. Ahmad, Adsorption mechanisms of removing heavy metals and dyes from aqueous solution using date pits solid adsorbent, *J. Hazard. Mater.* 176 (2010) 510–520.
- [3] P. Wu, T. Wu, W. He, L. Sun, Y. Li, D. Sun, Adsorption properties of dodecylsulfate-intercalated layered double hydroxide for various dyes in water. *Colloids Surf., A: Physicochem. Eng. Aspects* 436 (2013) 726–731.
- [4] A. Aziz, M.S. Ouali, E.H. Elandaloussi, L.C. De Menorval, M. Lindheimer, Chemically modified olive stone: A low-cost sorbent for heavy metals and basic dyes removal from aqueous solutions, *J. Hazard. Mater.* 163 (2009) 441–447.
- [5] G.M. Gadd, Biosorption: Critical review of scientific rationale, environmental importance and significance

- for pollution treatment, *J. Chem. Technol. Biotechnol.* 84 (2009) 13–28.
- [6] D. Park, Y.-S. Yun, J.M. Park, The past, present, and future trends of biosorption, *Biotechnol. Bioprocess Eng.* 15 (2010) 86–102.
- [7] A.P. Davis, M. Shokouhian, H. Sharma, C. Minami, D. Winogradoff, Water quality improvement through bioretention: Lead, copper, and zinc removal, *Water Environ. Res.* 75 (2003) 73–82.
- [8] E. Khosla, S. Kaur, P.N. Dave, Tea waste as adsorbent for ionic dyes, *Desalin. Water Treat.* 51 (2013) 6552–6561.
- [9] F. Ferrero, Adsorption of Methylene Blue on magnesium silicate: Kinetics, equilibria and comparison with other adsorbents, *J. Environ. Sci.* 22 (2010) 467–473.
- [10] V. Lugo-Lugo, C. Barrera-Díaz, F. Ureña-Núñez, B. Bilyeu, I. Linares-Hernández, Biosorption of Cr(III) and Fe(III) in single and binary systems onto pretreated orange peel, *J. Environ. Manage.* 112 (2012) 120–127.
- [11] A.B. Albadarin, C. Mangwandi, G.M. Walker, S.J. Allen, M.N.M. Ahmad, M. Khraisheh, Influence of solution chemistry on Cr(VI) reduction and complexation onto date-pits/tea-waste biomaterials, *J. Environ. Manage.* 114 (2013) 190–201.
- [12] G.Z. Kyzas, N.K. Lazaridis, M. Kostoglou, On the simultaneous adsorption of a reactive dye and hexavalent chromium from aqueous solutions onto grafted chitosan, *J. Colloid Interface Sci.* 407 (2013) 432–441.
- [13] G. Blázquez, M. Calero, F. Hernáinz, G. Tenorio, M.A. Martín-Lara, Batch and continuous packed column studies of chromium(III) biosorption by olive stone, *Environ. Prog. Sustainable Energy* 30 (2010) 576–585.
- [14] M.A. Martín-Lara, F. Hernáinz, M. Calero, G. Blázquez, G. Tenorio, Surface chemistry evaluation of some solid wastes from olive-oil industry used for lead removal from aqueous solutions, *Biochem. Eng. J.* 44 (2009) 151–159.
- [15] M.A. Martín-Lara, G. Blázquez, A. Ronda, A. Pérez, M. Calero, Development and characterization of biosorbents to remove heavy metals from aqueous solutions by chemical treatment of olive stone, *Ind. Eng. Chem. Res.* 52 (2013) 10809–10819.
- [16] M.A. Martín-Lara, G. Blázquez, M.C. Trujillo, A. Pérez, M. Calero, New treatment of real electroplating wastewater containing heavy metal ions by adsorption onto olive stone, *J. Cleaner Prod.* 81 (2014) 120–129.
- [17] G. Blázquez, M.A. Martín-Lara, E. Dionisio-Ruiz, G. Tenorio, M. Calero, Evaluation and comparison of the biosorption process of copper ions onto olive stone and pine bark, *J. Ind. Eng. Chem.* 17 (2011) 824–833.
- [18] M.A. Martín-Lara, G. Blázquez, A. Ronda, I.L. Rodríguez, M. Calero, Multiple biosorption-desorption cycles in a fixed-bed column for Pb(II) removal by acid-treated olive stone, *J. Ind. Eng. Chem.* 18 (2012) 1006–1012.
- [19] G. Blázquez, F. Hernáinz, M. Calero, M.A. Martín-Lara, G. Tenorio, The effect of pH on the biosorption of Cr(III) and Cr(VI) with olive stone, *Chem. Eng. J.* 148 (2009) 473–479.
- [20] A. Günay, E. Arslankaya, İ. Tosun, Lead removal from aqueous solution by natural and pretreated clinoptilolite: Adsorption equilibrium and kinetics, *J. Hazard. Mater.* 146 (2007) 362–371.
- [21] Langmuir, The adsorption of gases on plane surfaces of glass, mica and platinum, *J. Am. Chem. Soc.* 40 (1918) 1361–1403.
- [22] Freundlich, Über die adsorption in losungen, *Z. Phys. Chem.* 57 (1906) 385–470.
- [23] Y.S. Ho, G. McKay, The kinetics of sorption of divalent metal ions onto sphagnum moss peat, *Water Res.* 34 (2000) 735–742.
- [24] G. Blázquez, M.A. Martín-Lara, E. Dionisio-Ruiz, G. Tenorio, M. Calero, Copper biosorption by pine cone shell and thermal decomposition study of the exhausted biosorbent, *J. Ind. Eng. Chem.* 18 (2012) 1741–1750.
- [25] B. Zhao, Y. Shang, W. Xiao, C. Dou, R. Han, Adsorption of Congo red from solution using cationic surfactant modified wheat straw in column model, *J. Environ. Chem. Eng.* 2 (2014) 40–45.
- [26] Y.Y. Su, B.L. Zhao, W.W. Xiao, R.P. Han, Adsorption behavior of light green anionic dye using cationic surfactant-modified wheat straw in batch and column mode, *Environ. Sci. Pollut. Res.* 20 (2013) 5558–5568.